Strain smoothing technique in 3D for nearly incompressible neo-Hookean material

Chang-Kye Lee [*]   L. Angela Mihai [†]   Pierre Kerfriden[*]

Stéphane P.A. Bordas[*‡]

February 12, 2014

1   Introduction

Since strain smoothing approach, particularly smoothed finite element method (S-FEM) in FEM, was introduced, S-FEM has been highlighted due to its strengths, effectively alleviating volumetric locking and distorted meshes. Despite these positives, this approach is still remained in 2D and linear elasticity.

We provided remarkable results for volumetric locking with nearly incompressible neo-Hookean material in 2D using node-based S-FEM (NS-FEM) and edge-based S-FEM (ES-FEM). In this report, we extend S-FEM in 2D to 3D with face-based S-FEM (FS-FEM), and introduce NS-FEM in 3D. Benchmarking tests, simple shear and Lateral extension with Dirichlet and Neumann boundary conditions, and "Not-so-simple" shear deformation with

[*]Cardiff School of Engineering, Cardiff University, The Queen's Building, The Parade, Cardiff, Wales, CF24 3AA, UK.

[†]Cardiff School of Mathematics, Cardiff University, Senghennydd Road, Cardiff, Wales, CF24 4AG, UK.

[‡]Université du Luxembourg, Faculté des Sciences, de la Technologies et de la Communication, Campus Kirchberg, 6, rue Coudenhove-Kalergi, L-1359, Luxembourg.

Dirichlet boundadry conditions, are implemented and the accuracy and convergence of strain energy of proposed methods are provided.

2 Smoothed Finite Element Method

Face-based S-FEM (FS-FEM) Fig. 1 describes the smoothing domains for face-based smoothed finite element method (FS-FEM). The idea of this method is the same as ES-FEM, smoothing domains are associated to face instead of edge. Nodes 1,2,3 and 4 are element node, and node 5 is the centroid of tetrahedral element 1234.
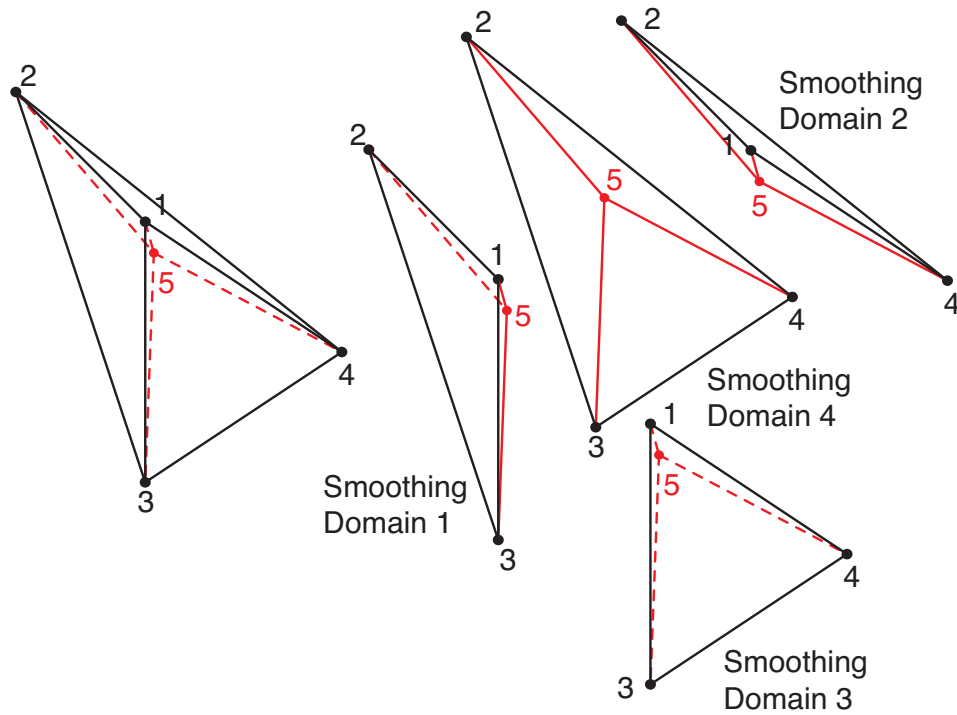

Figure 1: Smoothing domains for FS-FEM with tetrahedral element.
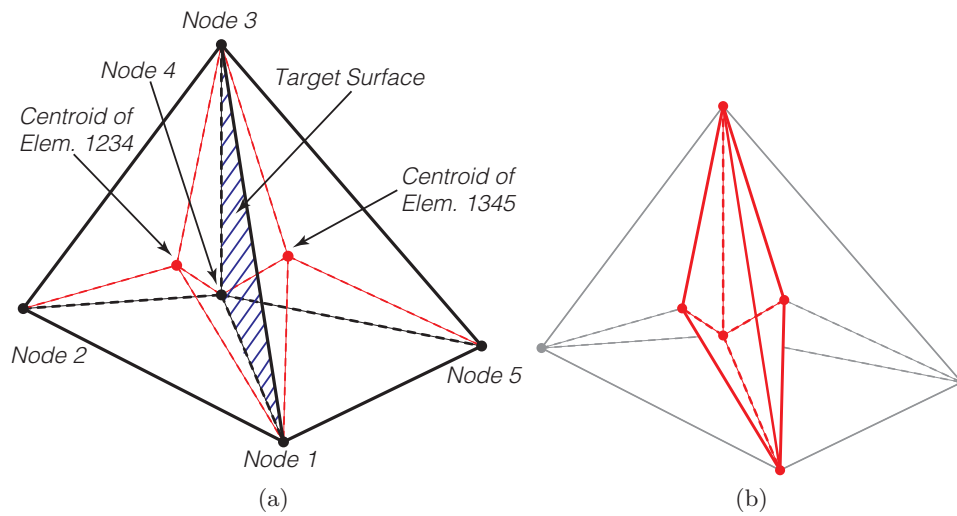
Figure 2: (a) Smoothing domains of FS-FEM with two tetrahedral elements (1234 and 1345) and those centroids; (b) Smoothing domains associated to target surface.

Node-based S-FEM (NS-FEM) Fig. 3 illustrates the numbering of element nodes and smoothing domain nodes, and four-smoothing domains for NS-FEM in 3D. In 2D, there are three-smoothing domains in triangular element; however, four-smoothing domains are generated for tetrahedral element in 3D. Nodes 1, 2, 3 and 4 in black are element nodes, and nodes 11, 12, 13 and 14 in blue are the centroid of $\triangle 123$, $\triangle 234$, $\triangle 124$ and $\triangle 134$, respectively. Node 15 in red is the centroid of tetrahedral element 1234.
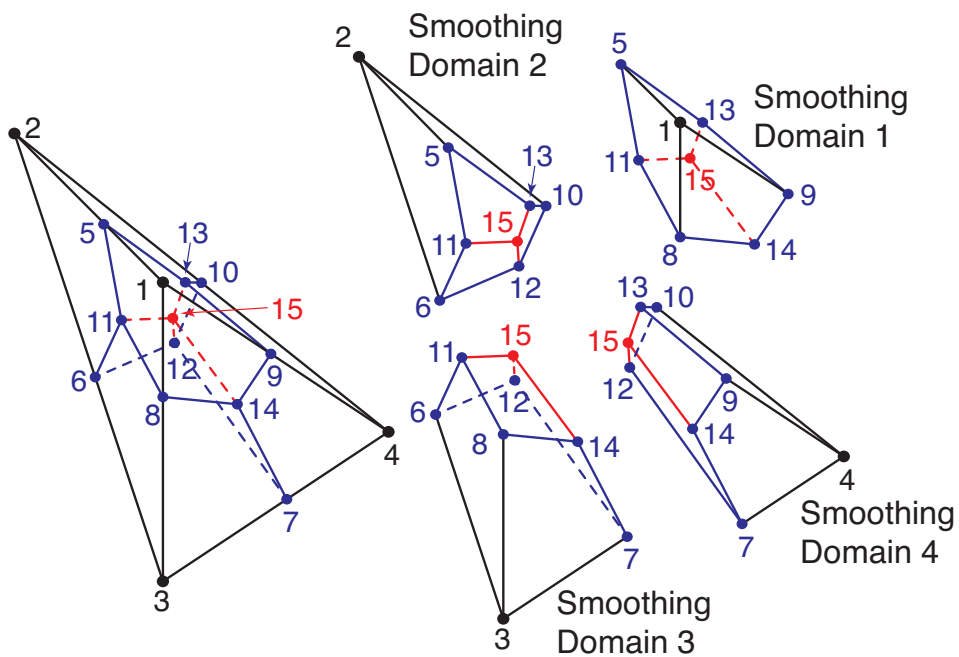
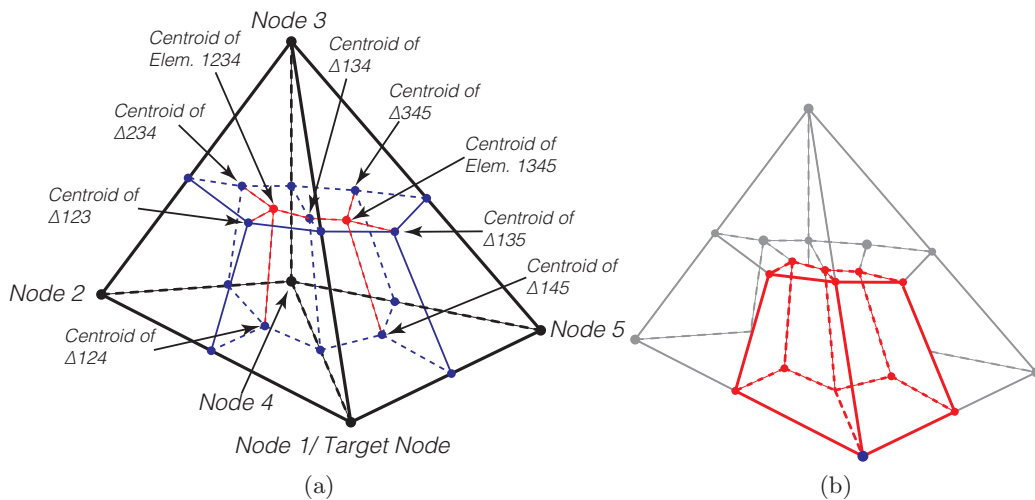Figure 3: Smoothing domains for NS-FEM with tetrahedral element.

(a)

(b)

Figure 4: (a) Smoothing domains of NS-FEM with two tetrahedral elements (1234 and 1345), and those smoothing domains; (b) Smoothing domains associated to target node.

4

3   Numerical examples

The stored energy function for a compressible neo-Hookean material is

$$W\left(\mathbf{C}\right) = \frac{1}{2}\lambda\left(\ln J\right)^2 - \mu\ln J + \frac{1}{2}\mu\left(\mathrm{tr}\mathbf{C} - 3\right) \tag{1}$$

where μ is the shear modulus and Lamé's first parameter λ is $\lambda = \kappa - \left(2/3\right)\mu$ where κ is the bulk modulus. For following bechmarking tests, the shear modulus $\mu = 0.6$ or $E = 1.7964$, and the bulk modulus $\kappa = 100$ or $\nu \approx 0.497$ are used.

For following tests, normal unit vectors to surfaces are given by:

- Top Surface: $(0, 1, 0)^{\mathrm{T}}$;

- Left Surface: $(-1, 0, 0)^{\mathrm{T}}$;

- Right Surface: $(1, 0, 0)^{\mathrm{T}}$;

- Front Surface: $(0, 0, -1)^{\mathrm{T}}$;

- Back Surface: $(0, 0, 1)^{\mathrm{T}}$.

3.1   Simple Shear

The deformation gradient for the simple shear is

$$\mathbf{F} = \begin{bmatrix} 1 & k & 0 \\ 0 & 1 & 0 \\ 0 & 0 & 1 \end{bmatrix} = \begin{bmatrix} 1 & 1 & 0 \\ 0 & 1 & 0 \\ 0 & 0 & 1 \end{bmatrix} \tag{2}$$

and the strain energy is

$$W = \frac{\mu}{2}k^2 = 0.3 \tag{3}$$

Dirichlet boundary conditions. Dirichlet boundary conditions for the simple shear are imposed:

- Bottom Surface: $(u_1, u_2, u_3) = (0, 0, 0)$;

- Top Surface: $(u_1, u_2, u_3) = (kX_2, 0, 0) = (1, 0, 0)$;

- Left- and Right-hand Surfaces: $(u_1, u_2, u_3) = (kX_2, 0, 0)$;

- Front and Back Surfaces: $(u_1, u_2, u_3) = (kX_2, 0, 0)$.

Fig. 5 describes the deformed shape of simple shear for Dirichlet and Neumann boundary conditions.
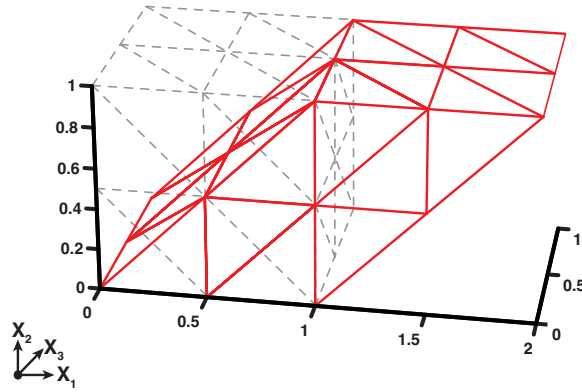

Figure 5: Deformed shape for simple shear with Dirichlet boundary conditions.

Fig. 6 shows the convergence of strain energies of FEM, FS-FEM and NS-FEM, and Table 1 provides the strain energy relative error. Errors of FEM, FS-FEM and NS-FEM are remarkably small; therefore, those errors are acceptable.
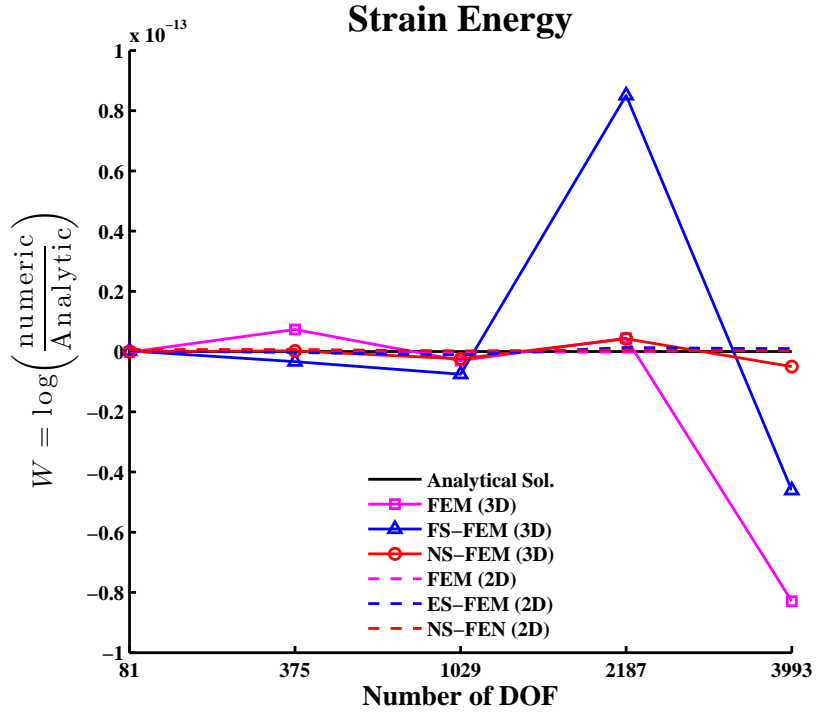
6

Figure 6: Strain energy convergence.

Table 1: Strain energy relative error $\left(\times 10^{-12}\%\right)$

Num. of DOFs	FEM		FS-FEM		NS-FEM	
	2D	3D	ES-FEM	FS-FEM	2D	3D
81	0.0000	-0.0019	0.0019	0.0019	0.0056	0.0000
375	0.0019	0.0722	-0.0037	-0.0333	0.0056	0.0019
1029	-0.0019	-0.0296	-0.0111	-0.0759	0.0019	-0.0241
2187	-0.0019	0.0444	0.0130	0.8493	0.0037	0.0426
3993	0.0111	-0.8290	0.0093	-0.4607	0.0019	-0.0500

Strain energy relative error is given by: $\left(\dfrac{W_{\text{Num.}} - W_{\text{Exact}}}{W_{\text{Exact.}}}\right) \times 100.$

7

Mixed boundary conditions. The first Piola-Kirchhoff stress tensor is

$$\mathbf{P} = \begin{bmatrix} \sigma_{11} - k\sigma_{12} & \sigma_{12} & 0 \\ \sigma_{12} - k\sigma_{22} & \sigma_{22} & 0 \\ 0 & 0 & \sigma_{33} \end{bmatrix} = \begin{bmatrix} 0 & k\mu & 0 \\ k\mu & 0 & 0 \\ 0 & 0 & 0 \end{bmatrix} = \begin{bmatrix} 0 & 0.6 & 0 \\ 0.6 & 0 & 0 \\ 0 & 0 & 0 \end{bmatrix} \quad (4)$$

The Dirichlet and Neumann boundary conditions are imposed as follows:

- Bottom Surface: $(u_1, u_2, u_3) = (0, 0, 0)$;

- Top Surface: $(P_1, y_2, y_3) = (-P_{12}, 0, 0)$;

- Left-hand Surface: $(P_1, u_2, u_3) = (-P_{12}, 0, 0)$;

- Right-hand Surface: $(P_1, u_2, u_3) = (P_{12}, 0, 0)$;

- Front Surface: $(P_1, u_2, u_3) = (P_{12}, 0, 0)$;

- Back Surface: $(P_1, u_2, u_3) = (-P_{12}, 0, 0)$.

Fig. 7 describes the deformed shape of simple shear with mixed boundary conditions, and fig. 8 illustrates the convergence of strain energy for FEM, FS-FEM and NS-FEM comparing an analytical solution.
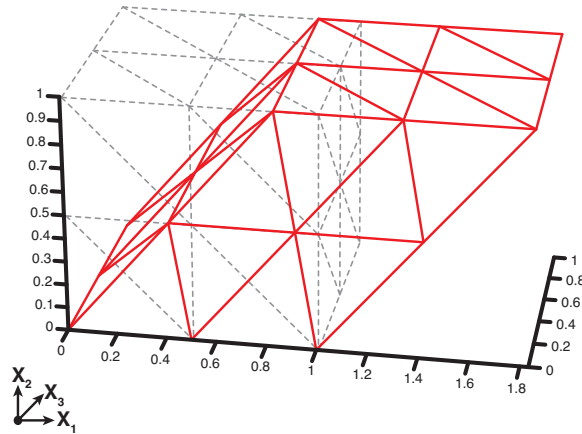

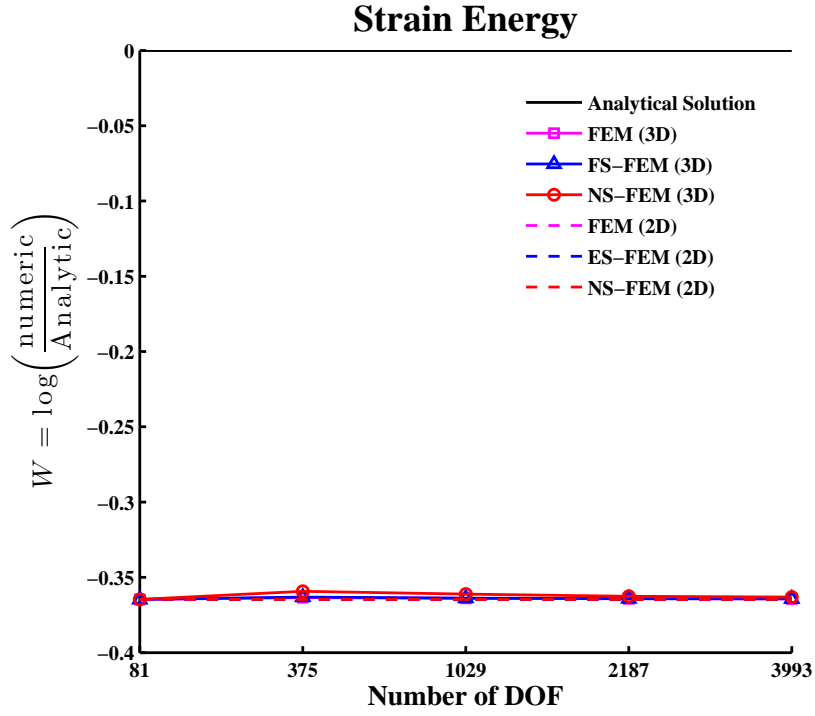Figure 7: Deformed shape for simple shear with mixed boundary conditions.

Figure 8: Strain energy convergence of FEM, FS-FEM and NS-FEM.

The strain energy relative errors are explained in Table 2. With mixed boundary conditions, errors of all methods are about 30%.

Table 2: Strain energy relative error (%)

Num. of DOFs	FEM		FS-FEM		NS-FEM	
	2D	3D	ES-FEM	FS-FEM	2D	3D
81	-30.5556	-30.5556	-30.5556	-30.5556	-30.5556	-30.5556
375	-30.5556	-30.4751	-30.5556	-30.4512	-30.5556	-30.1798
1029	-30.5556	-30.5087	-30.5556	-30.4973	-30.5556	-30.3085
2187	-30.5556	-30.5247	-30.5556	-30.5181	-30.5556	-30.4100
3993	-30.5556	-30.5339	-30.5556	-30.5296	-30.5556	-30.4504

Strain energy relative error is given by: $\left(\dfrac{W_{\mathrm{Num.}} - W_{\mathrm{Exact}}}{W_{\mathrm{Exact.}}} \right) \times 100.$

3.2 Uniform Extension with Lateral Contraction

The corresponding deformation gradient is

$$\mathbf{F} = \begin{bmatrix} \lambda_1 & 0 & 0 \\ 0 & \lambda_2 & 0 \\ 0 & 0 & \lambda_3 \end{bmatrix} = \begin{bmatrix} 1.15 & 0 & 0 \\ 0 & 0.869565217391304 & 0 \\ 0 & 0 & 1 \end{bmatrix} \tag{5}$$

Hence, we can get the strain energy for this test

$$W = \frac{\mu}{2}\left(\lambda_1^2 + \frac{1}{\lambda_1^2} - 2\right) = 0.023593100189036 \tag{6}$$

Dirichlet boundary conditions. The following Dirichlet boundary conditions are imposed:

- Bottom Surface: $(u_1, u_2, u_3) = ((\lambda_1 - 1)X_1, 0, 0) = (0.15X_1, 0, 0)$;

- Top Surface: $(u_1, u_2, u_3) = ((\lambda_1 - 1)X_1, (1/\lambda_1 - 1)X_2, 0)$
  $$= (0.15X_1, -0.130434782608696X_2, 0);$$

- Left-hand Surface: $(u_1, u_2, u_3) = (0, (1/\lambda_1 - 1)X_2, 0)$
  $$= (0, -0.130434782608696X_2, 0);$$

- Right-hand Surface: $(u_1, u_2, u_3) = ((\lambda_1 - 1), (1/\lambda_1 - 1)X_2, 0)$
  $$= (0.15X_1, -0.130434782608696X_2, 0);$$

- Front and Back Surfaces: $(u_1, u_2, u_3) = ((\lambda_1 - 1)X_1, (1/\lambda_1 - 1)X_2, 0)$
  $$= (0.15X_1, -0.130434782608696X_2, 0);$$

Fig. 9 illustrates the deformed shape of uniform extension with Dirichlet boundary conditions.
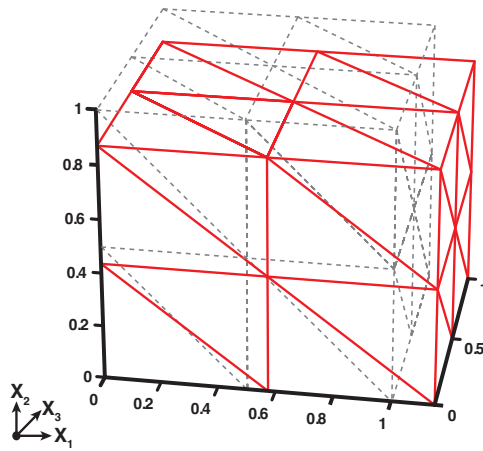
10

Figure 9: Deformed shape of uniform extension with Dirichlet boundary conditions.

The convergences of uniform extension for FEM, FS-FEM and NS-FEM are shown in fig. 10. Results of FS-FEM and NS-FEM are much more stable than FEM.
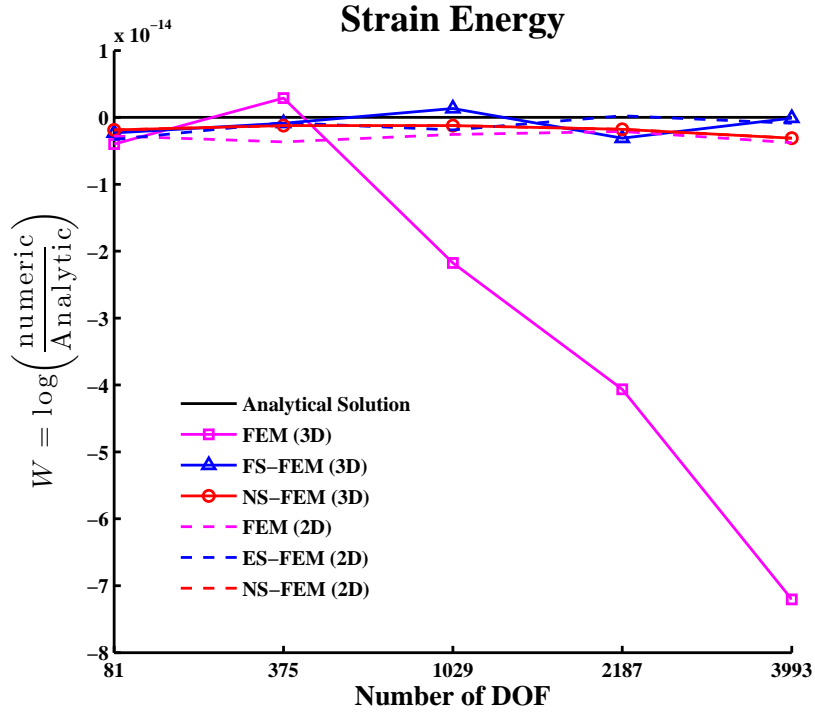
Figure 10: Strain energy convergence of uniform extension for FEM, FS-FEM and NS-FEM.

Table 3: Strain energy relative error $\left(\times 10^{-12}\%\right)$

Num. of DOFs	FEM		FS-FEM		NS-FEM	
	2D	3D	ES-FEM	FS-FEM	2D	3D
81	-0.0279	-0.0397	-0.0338	-0.0235	-0.0029	-0.0191
375	-0.0368	-0.0279	-0.0074	-0.0088	-0.0059	-0.0118
1029	-0.0250	-0.2176	-0.0191	-0.0132	-0.0147	-0.0118
2187	-0.0206	-0.4059	0.0029	-0.0309	-0.0103	-0.0176
3993	-0.0382	-0.7206	-0.0088	-0.0015	-0.0132	-0.0309

Strain energy relative error is given by: $\left(\dfrac{W_{\text{Num.}} - W_{\text{Exact}}}{W_{\text{Exact.}}}\right) \times 100.$

Mixed boundary conditions. The non-zero components for the first Piola-Kirchhoff stress are

$$
\begin{aligned}
P_{11} &= \frac{\sigma_{11}}{\lambda_1} = \mu\left(\lambda_1 - \frac{1}{\lambda_1}\right) = 0.168260869565217 \\
P_{22} &= -P_{11} = -0.168260869565217
\end{aligned}
\tag{7}
$$

The mixed boundary conditions are imposed as follows:

- Bottom Surface: $(P_1, u_2, u_3) = (P_{11}, 0, 0)$;

- Top Surface: $(P_1, u_2, u_3) = (P_{11}, P_{22}, 0)$;

- Left-hand Surface: $(u_1, P_2, u_3) = (0, P_{22}, 0)$;

- Right-hand Surface: $(P1, P_2, u_3) = (P_{11}, P_{22}, 0)$;

- Front and back surfaces: $(P_1, P_2, u_3) = (P_{11}, P_{22}, 0)$;
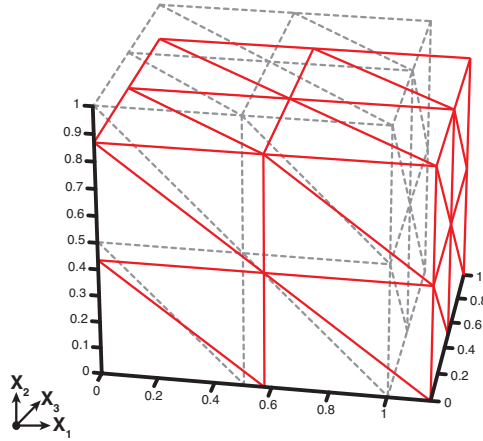

Figure 11: Deformed shape of uniform extension with mixed boundary conditions.

For this test, the errors of NS- and FS-FEM are relatively higher than those of FEM (Fig. 12); however these errors are still acceptable (Tabel 4).
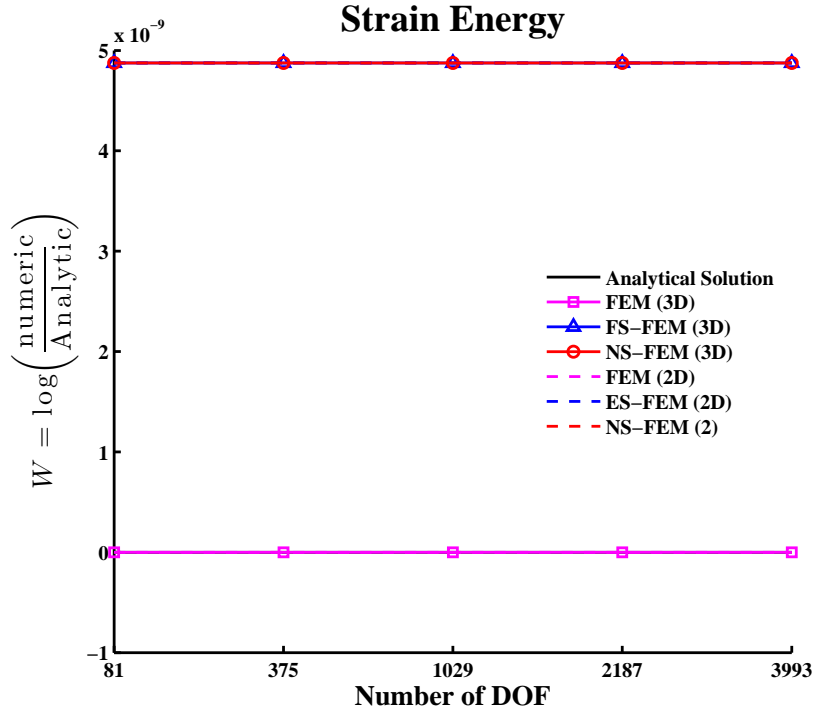
13

Figure 12: Strain energy convergence of uniform extension for FEM, FS-FEM and NS-FEM.

Table 4: Strain energy relative error (%)

Num. of DOFs	FEM$\left(\times 10^{-12}\right)$		FS-FEM$\left(\times 10^{-6}\right)$		NS-FEM$\left(\times 10^{-6}\right)$	
	2D	3D	ES-FEM	FS-FEM	2D	3D
81	-0.0735	-0.0662	0.4876	0.4875	0.4876	0.4876
375	-0.0529	-0.0029	0.4876	0.4875	0.4876	0.4875
1029	-0.0721	-0.2382	0.4876	0.4875	0.4876	0.4875
2187	-0.0897	-0.4220	0.4876	0.4875	0.4876	0.4875
3993	-0.0882	-0.7264	0.4876	0.4875	0.4876	0.4875

Strain energy relative error is given by: $\left(\dfrac{W_{\text{Num.}} - W_{\text{Exact}}}{W_{\text{Exact.}}}\right) \times 100.$

3.3 "Not-so-simple" shear

The non-homogeneous deformation gradient is

$$\mathbf{F} = \begin{bmatrix} 1 & 2kX_2 & 0 \\ 0 & 1 & 0 \\ 0 & 0 & 1 \end{bmatrix}, \quad X \in [0, 2] \tag{8}$$

and the strain energy is

$$W = \frac{\mu}{2} (2kX_2)^2 = 2\mu k^2 X_2^2 \tag{9}$$

Hence, Eq. 9 is

$$\begin{aligned} E = \int_V W \mathrm{d}X &= \int_0^2 \left(\int_0^2 \left(\int_0^2 2\mu k^2 X_2^2 \mathrm{d}X_2 \right) \mathrm{d}X_1 \right) \mathrm{d}X_3 \\ &= 4 \left(2\mu k^2 \left. \frac{X_2^3}{3} \right|_0^2 \right) = \frac{64}{3} \mu k^2 = 3.2 \end{aligned} \tag{10}$$

where $k = 0.5$.

Dirichlet boundary conditions. The following Dirichlet boundary conditions are imposed:

- Bottom Surface: $(u_1, u_2, u_3) = (0, 0, 0)$;

- Top Surface: $(u_1, u_2, u_3) = (2, 0, 0)$;

- Left- and Right-hand Surfaces: $(u_1, u_2, u_3) = (kX_2^2, 0, 0)$;

- Front and Back Surfaces: $(u_1, u_2, u_3) = (kX_2^2, 0, 0)$.

Fig. 13 shows the deformed shape of "Not-so-simple" shear deformation with Dirichlet boundary conditions.
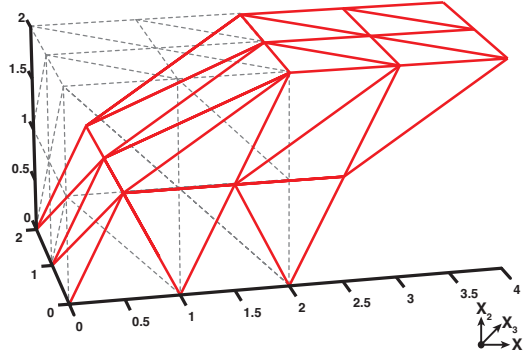
Figure 13: Deformed shape of "Not-so-simple" shear with Dirichlet boundary conditions.

(a) Convergence of strain energy (3D)
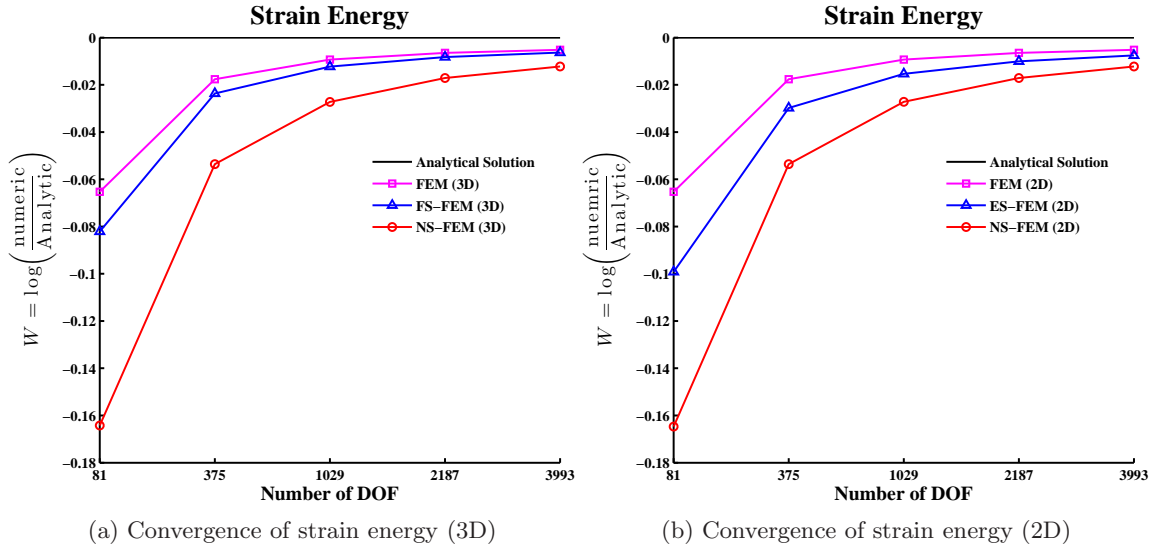
(b) Convergence of strain energy (2D)

Figure 14: Strain energy convergence of "Not-so-simple" shear of FEM, FS-FEM and NS-FEM: (a) Analytical strain energy is $W = 3.2$ in 3D; (b) Analytical strain energy is $W = 1.6$ in 2D.

For "Not-so-simple" shear deformation, the result of FEM is given upper bound solution for 2D and 3D. However, the convergence (Fig. 14) of NS- and FS-FEM for 3D is faster than 2D problems.

Table 5: Strain energy relative error (%)

Num. of DOFs	2D ($W = 1.6$)			3D ($W = 3.2$)		
	FEM	ES-FEM	NS-FEM	FEM	FS-FEM	NS-FEM
81	-6.3190	-9.4428	-15.1836	-6.3190	-7.8804	-15.1470
375	-1.7452	-2.9355	-5.2169	-1.7473	-2.3402	-5.2158
1029	-0.9250	-1.5214	-2.6853	-0.9267	-1.2227	-2.6860
2187	-0.6442	-1.0001	-1.6983	-0.6454	-0.8216	-1.6986
3993	-0.5162	-0.7523	-1.2150	-0.5170	-0.6338	-1.1251

Strain energy relative error is given by: $\left(\dfrac{W_{\text{Num.}} - W_{\text{Exact}}}{W_{\text{Exact.}}} \right) \times 100$.

4 Conclusions

In this report, we introduce 3D node-based Smoothed FEM, and some numerical examples are implemented. With analytical solutions of these tests, NS-FEM and FS-FEM show good performance and accurate results, compared to FEM and tests in 2D. As a future work, practical tests will be implemented, and we are looking forward to improved results rather than FEM.

References

[1] T. Belytschko, B. Moran and W.K. Liu. *Nonlinear finite element analysis for continua and structures*. Wiley, 1999.

[2] G.R. Liu and T.T. Nguyen. *Smoothed Finite Element Methods*. CRC Press, 2010.

[3] L.A. Mihai and A. Goriely. Numerical simulation of shear and the Poynting effects by the finite element method: An application of the generalised empirical inequalities in non-linear elasticity. *International JOurnal of Non-Linear Mechanics*, Vol. **49**, 1202–1211, 2013.